Optics Communications ■ (■■■■) ■■■–■■■

Contents lists available at ScienceDirect

Optics Communications

journal homepage: www.elsevier.com/locate/optcom

Numerical investigation of tunable Fano-based optical bistability in coupled nonlinear gratings

Quang Minh Ngo [a,*], Khai Q. Le [b], Thu Trang Hoang [a], Dinh Lam Vu [a], Van Hoi Pham [a]

[a] Institute of Materials Science, Vietnam Academy of Science and Technology, 18 Hoang Quoc Viet Road, Cau Giay, Hanoi, Vietnam
[b] Faculty of Science and Technology, Hoa Sen University, Ho Chi Minh City, Vietnam

ARTICLE INFO

Article history:
Received 13 September 2014
Received in revised form
2 November 2014
Accepted 4 November 2014

Keywords:
Gratings
Optical bistability
Integrated optics devices

ABSTRACT

In this paper, we numerically report the optical bistability based on tunable Fano resonances in photonic structures consisting of two coupled nonlinear slab waveguide gratings facing to each other. Quality factor (Q-factor) and asymmetric factor (q-factor) of Fano resonance of the coupled grating structure can be tuned by changing the gap-distance and horizontal shifted-alignment. The switching intensity not only depends on the Q-factor, but also strongly depends on the q-factor of the resonance. Considering strong coupling coefficients and optimizing the gap-distance between two gratings, the Fano resonance with high Q-factor and optimal q-factor can be excited. It is found that the horizontal shifted-alignment of the system provides high-order resonant mode having higher Q-factor and thus reduces the switching intensity than that of the perfect alignment system. Depending on the wavelengths of operation and q-factors of Fano resonances, the optical bistabilities will provide various switching intensities.

1. Introduction

Widespread attention has been drawn in all-optical bistable switching or bistability due to the implementation of all-optical information processing applications such as optical transistor, switches, logical gates, and memory for more than three decades from researchers in photonic fields [1–6]. It is expected to produce a new generation of photonic devices for various applications in telecommunication and information technology. The all-optical bistable switching provides almost fundamental functions, expected to play an important role in high-data-rate optical processing and does not require electrical-to-optical conversion. So that, it can solve the current problems of the microprocessors, network routers, and data centers, etc. In addition, all-optical switching devices do not either consume much energy or generate heat when operating at high-bit-rate which are ideal for next-generation environment-friendly devices [5–12]. The realization of the optical bistability at low input intensity has initiated a platform for the development of advanced chip-scale photonic networks. To enable the optical bistability at low switching intensity, the strong light-matter interaction is needed to enhance nonlinear effects of the structure. Various optical resonant designs and nonlinear materials and have been proposed to realize all-optical bistable switching devices. While natural materials normally have weak third-order nonlinear coefficients, properly forming them in particular structures such as high Q-factor cavities will create qualitatively strong nonlinearities. Usually, in order to reduce the optical switching intensity which requires a small resonant wavelength (frequency) shift, a high Q-factor resonator with narrow linewidth in the spectral response is needed [13–17]. Among all the proposed optical resonant structures, all-optical bistable devices based on guided-mode resonances in nonlinear slab waveguide gratings are promising designs due to their simple structures with easy in/out coupling and their cost-efficient fabrication process. Guided-mode resonances in nonlinear slab waveguide gratings have been designed and studied to get the different resonant shapes, but Fano resonance is an anomalous phenomenon which applied for efficient all-optical bistable switching due to its shape and asymmetric resonant profiles [18–24]. In such system, the spectral response can vary from 0 to 1 in a short wavelength range narrower than the full width of the resonance itself. Therefore it requires a small resonant shift to obtain a low switching intensity for optical bistability. In previous work, we have investigated the all-optical bistable switching based on Fano resonances in the single- and double-layer nonlinear slab waveguide gratings with narrow slits [20]. In the reflection spectrum of the double-layer slab waveguide gratings, there are two resonant peaks at short (F1) and longer (F2) resonant wavelengths. We have also demonstrated that the proposed double-layer slab waveguide gratings provided high all-optical bistable switching efficiency in terms of low switching intensity and high contrast of low and high

* Corresponding author.
E-mail addresses: minhnq@ims.vast.ac.vn (Q.M. Ngo), khai.lequang@hoasen.edu.vn (K.Q. Le).

http://dx.doi.org/10.1016/j.optcom.2014.11.017
0030-4018/

states at the F2 resonance. Its resonant characteristics strongly depend on the gap-distance between two slab waveguide gratings or the sandwiched layer thickness. In a different note, widely tunable resonant characteristics and Q-factors of two coupled photonic crystal slab structures were proposed [25–28]. These works have mainly treated the effect of configuration changes in the gap-distance and horizontal shifted-alignment to the Fano resonances. Several applications of this Fano-based structure have been introduced such as Fano resonant filters [25–27], energy conversion [28], etc… It can avoid the limited dispersion engineering capabilities for fine-tuning spectral responses compared to the single slab waveguide grating. In addition, this structure gives a wideband tuning range and allows controlling the structure parameters and upstanding design.

Based on the concept of tunable Fano resonances, in this paper, we investigate their optical bistabilities. The investigated structure consists of two identical nonlinear slab waveguide gratings facing to each other. Considering the subwavelength gap-distance between two slab waveguide gratings in the case of perfect alignment, two separated Fano resonances are excited to form the F1 and F2 resonances. We concentrate our interest in the Q-factors and shapes of the F2 resonance. Since the Q-factor of the coupled grating system is very sensitive to the horizontal shifted-alignment [26,27], we design the structure by fixing the optimal gap-distance and changing the horizontal shifted-alignment to get the F2 and high-order F2 resonances having higher Q-factors than that of the perfect alignment case. The optical bistability will be treated with emphasis on the F2 and high-order F2 Fano resonances. The high-order F2 Fano resonance provides higher Q-factor and lower switching intensity compared to the F2 resonance. Depending on the operating wavelength, we can tune the switching intensity of bistable behavior. In addition, our designed structures result in the Fano-based optical bistability in a wider bandwidth of operation than Lorentzian guided-mode resonances in slab waveguide gratings due to the tunable features of the asymmetric factor of Fano resonance. All simulations were carried out by the finite-difference time-domain method with subpixel smoothing for increased accuracy [29,30].

2. Optical bistability in coupled slab waveguide gratings

The schematic of two coupled identical slab waveguide gratings facing each other with a gap-distance of d and horizontal shifted-alignment of s is shown in Fig. 1. Each slab waveguide grating supports the Fano resonance, where key structural parameters are defined as the guiding layer made of chalcogenide glass (As_2S_3, $n=2.38$) with a thickness (h) of 220 nm on a thick glass substrate ($n=1.5$). The grating slit aperture (w) is formed by a rectangular corrugation in As_2S_3 guided layer with the depth and periodicity (Λ) of 220 nm and 860 nm, respectively. A normally incident plane wave with transverse electric (TE) (the electric field is parallel to the chalcogenide strip) polarization is used. Perfectly matched absorbing boundary conditions are applied for the top and bottom boundaries of the computational unit cell while periodic boundary conditions are set at the left and right boundaries [29]. Since the Q-factor of Fano resonance in coupled slab waveguide gratings is very sensitive to the gap-distance d and horizontal shifted-alignment s, we treat the Fano resonance in both cases of changing the gap-distance d and horizontal shifted-alignment s as follows:

2.1. Perfect alignment

In the case of perfect alignment ($s=0$) of two identical slab waveguide gratings, the coupling strength (determines Q-factor) and resonant wavelength of the system can be easily tuned by

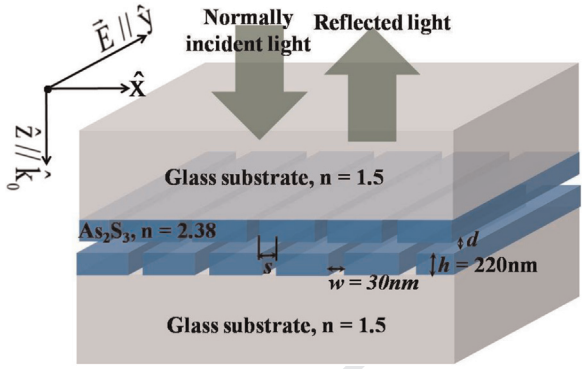

Fig. 1. Sketch of coupled slab waveguide gratings under normally incident light. The gap-distance d and horizontal shifted-alignment s are tuned for exciting Fano resonances.

changing the gap-distance d. As discussed in [20], when two slab waveguide gratings are coupled, there are two resonant wavelengths that we called first (F1) and second (F2) Fano resonances. Because of our interest focusing on the F2 shape, Fig. 2(a) shows the reflection spectra at F2 for various the gap-distances d. The gap-distance d is optimized to have the peak (maximum reflection) and depth (minimum reflection) at the resonance close to 1 and 0, respectively. The gap-distance d is important because the photons can tunnel between them and then the scattering effect will happen. As a result, the peak and depth will be not perfect unity and zero in some cases due to scattering loss [27]. This mechanism, therefore, no longer requires the long gap-distance d to achieve high reflectivity and sensitivity. For the grating width $w=30$ nm, the gap-distance d ($d \leq 300$ nm) is found close to an optimal value. In other words, for a gap-distance d as small as 300 nm, the Fano resonances with high sensitivity can be still existed. As increasing the gap-distance d, the F2's resonant peak shifts to the short wavelength and its Q-factor increases. The Q-factor of each resonance is estimated by fitting the calculated reflections using the Fano resonant lineshape as given in [19]:

$$R(\varepsilon) = F\frac{(\varepsilon + q)^2}{1 + \varepsilon^2} \quad (1)$$

where $\varepsilon = 2(2\pi c(1/\lambda - 1/\lambda_0))/\Gamma$, q is an asymmetric factor (q-factor), c is speed of light, λ_o is a resonant wavelength, F is constant factor, and Γ is the resonant linewidth at half maximum (FWHM). The resonant wavelength may lie somewhere in between the peak and the depth of the asymmetric lineshape, depends on the value of asymmetric factor q. The Q-factor is defined by the ratio between the resonant wavelength λ_o and Γ. The resonant peaks, estimated Q-factors, q-factors, and F factors for F2 resonances of the perfect alignment coupled two slab waveguide gratings for various gap-distances d are shown in Table 1. With the gap-distance 50 nm $\leq d \leq$ 300 nm, the resonant wavelengths are in the 1552.2–1684.9 nm range. The Q-factor increases as the gap-distance d increases due to the long distance of Fabry–Perrot (FP) resonator formed between two slab waveguide gratings [27]. High FP resonator's Q-factor makes leaky modes from the outside hard to couple into the resonator. It means that as the gap-distance d increases, the FP mode gets little leaky and hence the linewidth becomes narrower leading to an increase of Q-factor. The Q-factors are 2104, 2543, 3759, and 8522 for the gap-distance d of 50 nm, 100 nm, 170 nm, and 300 nm, respectively. Further importance, as gap-distance d increases, the asymmetric factor q decreases and the reflectivity of side-bands (RSB) increases due to the strongly transition to the continuum. Hence, q-factor becomes a function of the RSB and Q-factor, $q \rightarrow q$(RSB,Q-factor). Our concentration

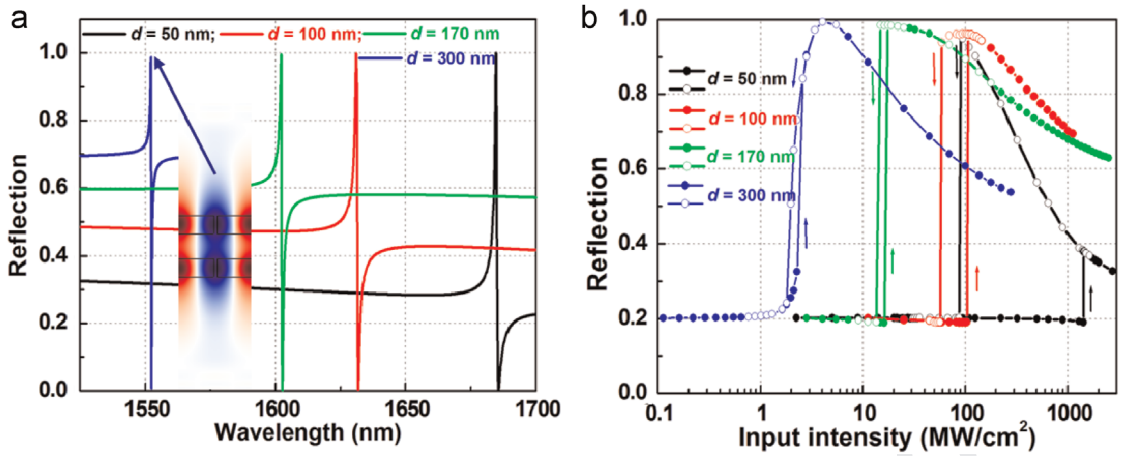

Fig. 2. (a) Reflection spectra of the coupled slab waveguide gratings depicted in Fig. 1 with $s=0$. The calculations are done for TE polarized light where electric-field is parallel to the chalcogenide strips. The inset shows field distribution at F2 resonance. (b) Bistability curves of the coupled gratings for various gap-distances d of 50 nm, 100 nm, 170 nm, and 300 nm, respectively, with operating wavelength at 20% reflection.

focuses on the positive asymmetric factor q as small as possible. The exact definition for q-factor is not easy to find in the arbitrary photonic systems.

Based on the linear spectra, the operating wavelength of optical bistability is chosen at 20% reflection. In general, the operating wavelength is chosen to the presence of bistable behavior, which was discussed in [20,24]. The bistable behaviors are calculated by measuring a reflected flux intensity of the CW source through on the substrate of slab waveguide grating. The reflected flux intensity is measured at the steady state. The low- (dotted solid curve) and high-reflection (dotted hollow curve) states are observed by increasing and decreasing the amplitude of the CW source, respectively. In nonlinear calculations, the third-order nonlinear coefficient of As_2S_3 is $n_2=3.12\times10^{-18}$ m^2/W [31]. Fig. 2 (b) shows the calculated bistable behaviors of the perfect alignment coupled slab waveguide gratings for the gap-distance d of 50 nm, 100 nm, 170 nm, and 300 nm. Bistable behaviors are clearly observed. In each bistable curve, the incident intensity for switching can be estimated as the input intensity for which the reflection increases abruptly in the dotted solid curve. The estimated switching intensities are 1427.1 MW/cm^2, 104.1 MW/cm^2, 16.2 MW/cm^2, and 2.2 MW/cm^2 corresponding to the quality factors $Q=2104$, 2543, 3759, and 8522, and asymmetric factor $q=1.609$, 1.110, 0.835, and 0.655 for the gap-distances $d=50$ nm, 100 nm, 170 nm, and 300 nm, respectively. In contrast to the Lorentzian resonance, these Fano-based results do not follow the $1/Q^2$ dependence rule of the switching intensity [13–17]. The switching intensity is also influenced by the asymmetric factor q. The asymmetric factor q relates to the Q-factor and the reflectivity of the side-bands. For example, the Q-factors and switching intensities are (2104, 1427.1 MW/cm^2), (2543, 104.1 MW/cm^2), and (8522 and 2.2 MW/cm^2) for the gap-distances d of 50 nm, 100 nm, and 300 nm, respectively. While the Q-factors increase gradually, the switching intensities dramatically decrease due to a reduction of asymmetric factors q. The Q-factor increases 4.0 times but the switching intensity decreases 648.7 times. The temporal responses on the Q-factors are not investigated here, which have shown the same tendency that we presented before [13,15].

We next consider the operating wavelength influence on the switching intensity. We keep the gap-distance d of 300 nm, the optical bistable behaviors for operating wavelengths at 20%, 30%, 40%, 50%, and 60% reflections corresponding to the shifted-wavelength ($\Delta\lambda$) of 0.088 nm, 0.143 nm, 0.222 nm, 0.367 nm, and 0.833 nm from the depth. As seen in Fig. 3, the switching intensities are 2.2 MW/cm^2, 4.4 MW/cm^2, 9.7 MW/cm^2, 20.6 MW/cm^2, and 140.5 MW/cm^2 for the operating wavelengths at 20%, 30%, 40%, 50%, and 60% reflections, corresponding to the operating wavelengths of 1552.319 nm, 1552.374 nm, 1552.453 nm, 1552.598 nm, and 1553.064 nm, respectively. It is seen that as we change the operating wavelength ($\Delta\lambda=0.745$ nm) from 20% to 60% reflections, the switching intensity increases from 2.2 MW/cm^2 to 140.5 MW/cm^2 (increasing 63.9 times). The bistable behaviors for the operating wavelengths at 10% and 0% (at the depth) are not shown here, show the same tendency as we discussed before [20]. The optical bistability based on Lorentzian shape, the operating frequency (or wavelength) should be detuned from a center frequency according to$(\omega_o-\omega)\tau>\sqrt{3}$ for existence of bistability, where τ is photon life time. It is found that the spectral range is from ~25% to 0% for Lorentzian lineshape [13–15] and from 0% to ~70% for Fano lineshape shown here, as an evidence for the wider bandwidth of operation to enable the optical bistability.

2.2. Horizontal shifted-alignment

Next, we consider coupled slab waveguide gratings with horizontal shifted-alignment. Various shifted-alignment coefficients s are examined while the gap-distance d of 300 nm is fixed as an optimal value to achieve the Fano resonance with high sensitivity and high Q-factor. Our calculated linear reflection spectra for the gratings with various horizontal shifted-alignments $s=100$ nm, 150 nm, and 430 nm as shown in Fig. 4(a). For comparison purpose, the linear reflection spectrum of coupled slab waveguide gratings with perfect alignment is also plotted. The horizontal

Table 1
Resonant peaks and Q-factors of the coupled slab waveguide gratings for various gap-distances d.

Gap-distance d (nm)	50	100	170	250	300
Resonant peak (nm)	1684.9	1631.4	1602.4	1573.1	1552.2
Q-factor	2104	2543	3759	6304	8522
q-factor	1.696	1.110	0.835	0.686	0.655
Switching intensity (MW/cm^2)	1427.1	104.1	16.2	4.6	2.2

Please cite this article as: Q.M. Ngo, et al., Optics Communications (2014), http://dx.doi.org/10.1016/j.optcom.2014.11.017

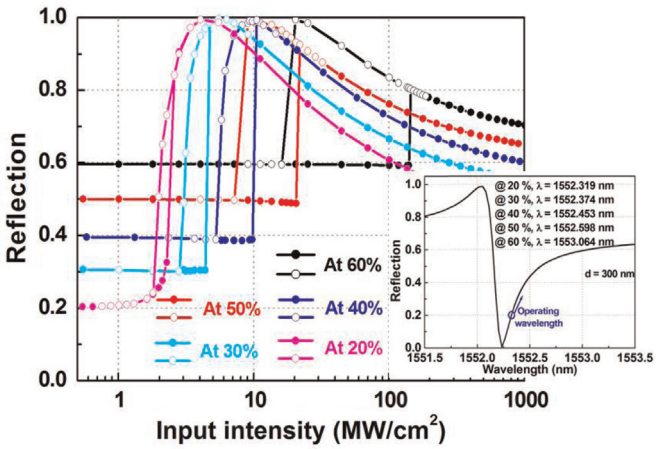

Fig. 3. Bistability behaviors for the gap-distance $d=300$ nm. The switching intensities are 2.2 MW/cm^2, 4.4 MW/cm^2, 9.7 MW/cm^2, 20.6 MW/cm^2, and 140.5 MW/cm^2 for the operating wavelengths at 20%, 30%, 40%, 50%, and 60% reflections, respectively.

shifted-alignment s is supposed to mainly change the phase retardation between two slab waveguide gratings. If horizontal shifted-alignment s is 430 nm (half-period), the reflection spectrum is reversed to the case of perfect alignment. So it may cause a phase retardation change of π. The deviations from either of the coupled slab waveguide gratings lead to high Q-factors' states [26]. In our case, we consider the horizontal shifted-alignment s of 100 nm and 150 nm and the reflection spectra are plotted in Fig. 4(a). There are four resonant peaks in each reflection spectrum of horizontal shifted-alignment s of 100 nm and 150 nm. The reflectivity of side-bands for all cases of perfect and horizontal shifted-alignment does not change. The reflectivity of side-bands is fixed at around 70%. There exist two Fano resonant F2 shapes, as shown in Fig. 4(b). The F2 and high-order F2 of Fano resonances are located at the longer and shorter wavelengths, respectively. The field distributions and Q-factors at resonances are shown in the insets of Fig. 4(b). As the results, the mirror symmetry of the system is broken and brings mainly change in the phase retardation between slab waveguide gratings. It results the higher Q-factors. Comparing the field distributions of the perfect alignment (inset of Fig. 2(a)) and the horizontal shifted-alignment cases (insets of Fig. 4(b)), we note that the horizontal shifted-alignment allows the excitation of the state of high-order F2 with a different local modal profile of F2. As seen in Fig. 4(b), the Q-factor of high-order F2 resonance is higher than that of F2 resonance. The Q-factors for F2 and high-order F2 are 12,187 and 51,733 for the horizontal shifted-alignment $s=100$ nm, and the Q-factors for F2 and high-order F2 are 15,596 and 32,738 for the horizontal shifted-alignment $s=150$ nm. Table 2 summarizes the linear characteristics of Fano resonances for the horizontal shifted-alignments $s=100$ nm and 150 nm of coupled slab waveguide gratings. The inset of Fig. 4(b) shows the electric field distributions at F2 and high-order F2 resonances.

The optical bistable behaviors for various operating wavelengths of the high-order F2 and F2 resonances in the case of the horizontal shifted-alignment $s=100$ nm are shown in Fig. 5(a) and (b), respectively. As seen in Fig. 5(a), the high-order F2 case, the switching intensities are 0.06 MW/cm^2, 0.10 MW/cm^2, 0.19 MW/cm^2, 0.59 MW/cm^2, and 4.43 MW/cm^2 for operating wavelengths at 20%, 30%, 40%, 50%, and 60% reflections. It is approximately two orders increasing of switching intensity when operating wavelength changes from 20% to 60%. In Fig. 5(b), for the F2 case, 1.08 MW/cm^2, 1.80 MW/cm^2, 3.43 MW/cm^2, 10.62 MW/cm^2, and 79.97 MW/cm^2 for operating wavelengths at 20%, 30%, 40%, 50%, and 60% reflections are shown. From Fig. 5(a) and (b), the high-order F2 and F2 resonances based the horizontal shifted-alignment, for the operating wavelength at certain reflection, the switching intensity is proportional to $1/Q^2$. For example, the operating wavelength at 20% refection, Q-factors and switching intensities are (12,187 and 1.08 MW/cm^2) and (51,733 and 0.06 MW/cm^2) for the F2 and high-order F2 resonances, respectively. At the F2 resonance, the Q-factor is 4.24 times smaller and the switching intensity is 18.0 times higher than those at high-order F2 resonances. In case of operating wavelength at 60% refection, the switching intensity at the F2 resonance is 79.97 MW/cm^2. It is 18.95 times higher than that at the high-order F2 resonances corresponding to the switching intensity of 4.43 MW/cm^2. Other operating wavelengths show the same tendency as shown in Table 2.

The above calculations were assumed with horizontal shifted-alignment s of 100 nm. However featured benefit of the coupled slab waveguide grating structure with horizontal shifted-alignment is the ability to increase the Q-factor. The bistable behaviors of the coupled slab waveguide gratings with horizontal shifted-alignment s of 150 nm are also treated. Fig. 6(a) and (b) show the bistable behaviors at high-order F2 and F2 Fano resonances. The switching intensities for operating wavelengths at 20%, 30%, 40%, 50%, and 60% are noted in Table 2. They are the same tendency as the results as shown in Fig. 5(a) and (b). The switching intensity is proportional to $1/Q^2$. Since the Q-factors and switching intensities accordingly of the coupled nonlinear gratings are dependent on the horizontal

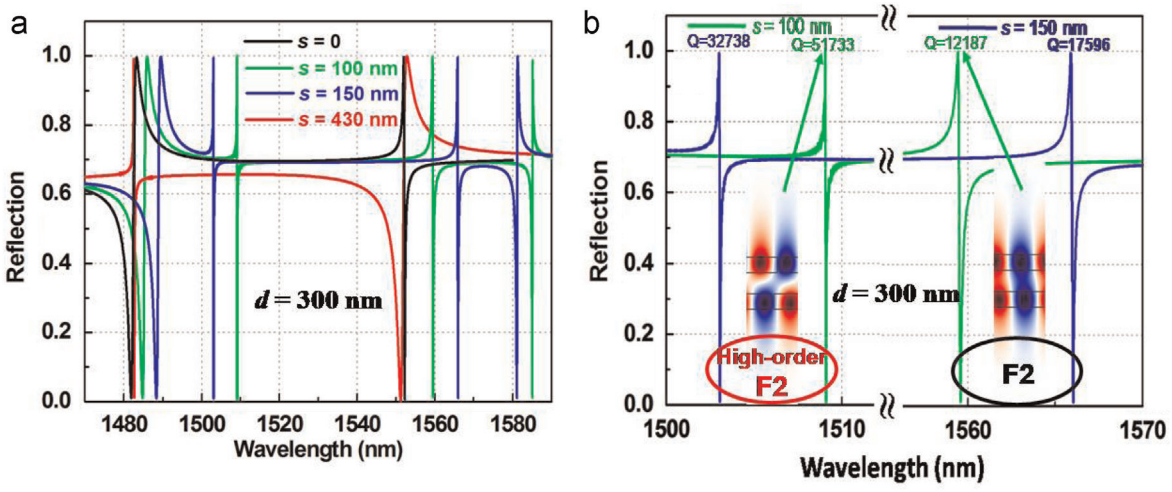

Fig. 4. (a) Full reflection spectra of the coupled slab waveguide grating for various horizontal shifted-alignments and (b) the enlarged F2 regions for horizontal shifted-alignments s of 100 nm and 150 nm. The gap-distance d is fixed at 300 nm.

Please cite this article as: Q.M. Ngo, et al., Optics Communications (2014), http://dx.doi.org/10.1016/j.optcom.2014.11.017

Table 2
The Q-factors and switching intensities for the horizontal shifted-alignment $s=100$ nm and 150 nm of the coupled slab waveguide gratings for high-order F2 and F2 Fano resonances.

		Shifted-alignment $s=100$ nm		Shifted-alignment $s=150$ nm	
		High-order F2	F2	High-order F2	F2
Q-factor		**51,733**	**12,187**	**32,738**	**17,586**
Switching intensity (MW/cm^2)	20%	**0.06**	**1.08**	**0.14**	**0.55**
	30%	**0.10**	**1.80**	**0.27**	**1.08**
	40%	**0.19**	**3.43**	**0.52**	**2.10**
	50%	**0.59**	**10.62**	**1.35**	**5.50**
	60%	**4.43**	**79.97**	**9.30**	**38.0**

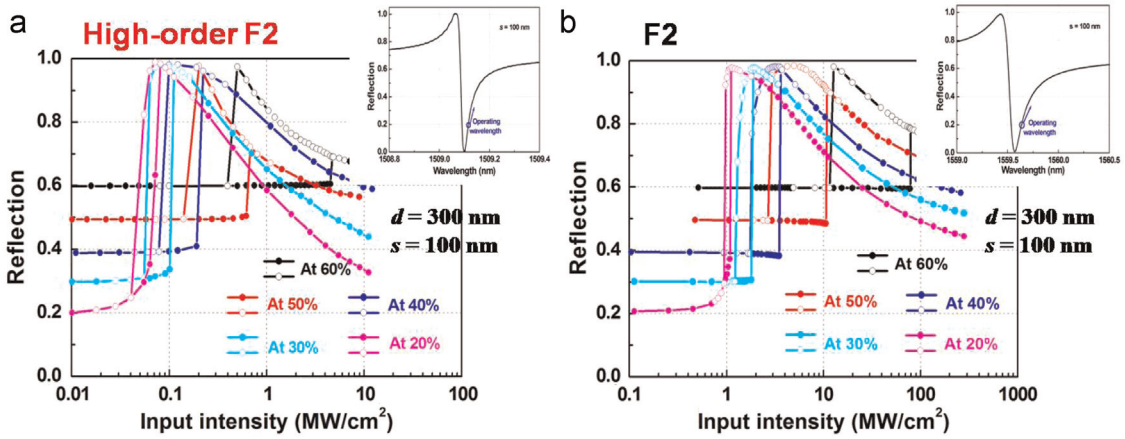

Fig. 5. The bistability behaviors of high-order F2 (a) and F2(a) resonances for various operating wavelengths of the coupled slab waveguide gratings for the horizontal shifted-alignment s of 100 nm.

shifted-alignment. In this work, we do not pay much attention on the optimization to achieve the highest Q-factor and lowest switching intensity. We instead focus on demonstrating the possibility to significant enhance the Q-factor and reduce the switching intensity by using the horizontal shifted-alignment. Based on the enhancement of Q-factor and reduce switching intensity accordingly by the horizontal shifted-alignment, the system will undoubtedly facilitate the development of new optical bistable devices towards high efficiency of switching intensity.

In this work, we assume the ideal device can be fabricated. The proposed coupled grating structures can be fabricated as the following procedures: (i) two single gratings can be fabricated first using electron-beam (e-beam) lithography and inductively coupled plasma etching (ICP) techniques. In particular, each grating having the As_2S_3 thin film with thickness of 220 nm is deposited on a glass substrates using RF/DC sputtering techniques [32]. To fabricate grating structure, the film is coated by an e-beam resist layer with a thickness of ~300 nm. The grating with the slit width and periodicity of 30 nm and 860 nm, respectively, is patterned on the e-beam resist layer by an e-beam lithography system. The sample is then etched by an ICP dry etcher using a mixture of CHF_3 and O_2 gases. The device structure is finally formed after removing the e-beam resist layer; (ii) coupled gratings via gap-distance and the horizontal shifted-alignment can be controlled by means of micro/nano-electromechanical systems (M/NEMS) [33,34]. Our proposed design here looks simple and more advantage than the previous one [20] in fabrication, which can reduce the unwanted shape of gratings when the gap-distance d thick. Other advantages are in easy controlling the gap-distance d and the horizontal shifted-alignment s.

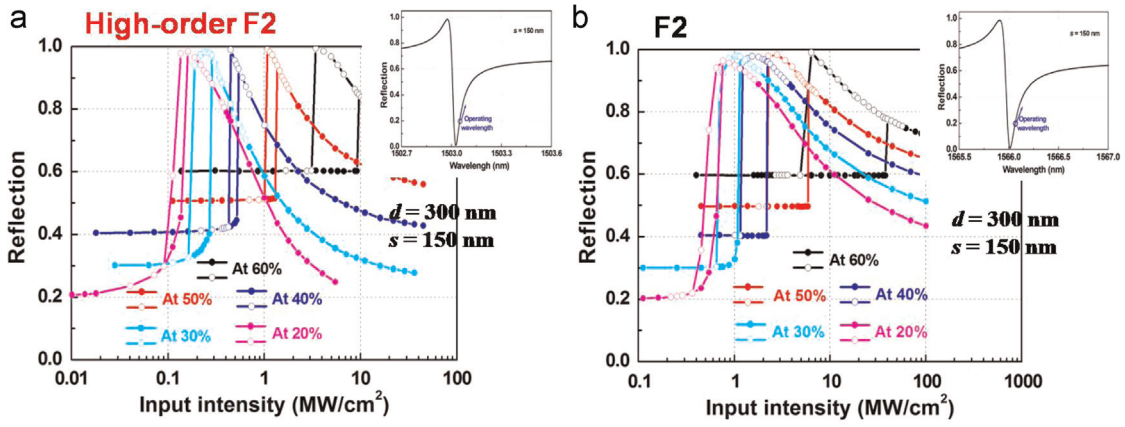

Fig. 6. Similar to Fig. 5 but for $s=150$ nm.

3. Conclusion

In conclusion the optical bistability has been observed in coupled nonlinear slab waveguide gratings. The proposed bistable structure operates at tunable Fano resonances with high *Q*-factors over a wider bandwidth of operation under low switching intensities. We believe that our designed structures and numerical results provide a useful guideline to realize efficient optical bistable devices.

Acknowledgments

This research is funded by Vietnam's National Foundation for Science and Technology Development (NAFOSTED) under grant number "103.03-2013.01".

References

[1] H.M. Gibbs, S.L. McCall, T.N.C. Venkatesan, Phys. Rev. Lett. 36 (1976) 1135.
[2] J.L. Jewell, H.M. Gibbs, A.C. Gossard, A. Passner, Wiegmann, Mater. Lett. 1 (1983) 148.
[3] H.M. Gibbs, Optical Bistability: Controlling Light with Light, Academic, 1985.
[4] E. Garmire, S.D. Allen, J. Marburger, C.M. Verber, Opt. Lett. 3 (1978) 69.
[5] M. Haurylau, G. Chen, H. Chen, J. Zhang, N.A. Nelson, D.H. Albonesi, E. G. Friedman, P.M. Fauchet, IEEE J. Sel. Top. Quant. Electron. 12 (2007) 1699.
[6] M. Notomi, A. Shinya, K. Nozaki, T. Tanabe, S. Matsuo, E. Kuramochi, T. Sato, H. Taniyama, H. Sumikura, IET Circuit Device Syst. 5 (2011) 84.
[7] K. Nozaki, T. Tanabe, A. Shinya, S. Matsuo, T. Sato, H. Taniyama, M. Notomi, Nat. Photon. 4 (2010) 477.
[8] D.A.B. Miller, Proc. IEEE 97 (2009) 1166.
[9] A. Shacham, K. Bergman, L.P. Carloni, IEEE Trans. Comput. 57 (2008) 1246.
[10] D.A.B. Miller, Int. J. Optoelectron. 11 (1997) 155.
[11] A.F. Benner, M. Ignatowski, J.A. Kash, D.M. Kuchta, M.B. Ritter, IBM J. Res. Dev. 49 (2005) 755.
[12] D.A.B. Miller, H.M. Ozaktas, J. Parallel Distrib. Comput. 41 (1997) 4252.
[13] Q.M. Ngo, S. Kim, S.H. Song, R. Magnusson, Opt. Express 17 (2009) 23459.
[14] Q.M. Ngo, T.T. Hoang, V.L. Nguyen, D.L. Vu, V.H. Pham, J. Opt. 15 (2013) 055503.
[15] Q.M. Ngo, S. Kim, J. Lee, H. Lim, J. Lightwave Technol. 30 (2012) 3525.
[16] M. Soljacic, M. Ibanescu, S.G. Johnson, Y. Fink, J.D. Joannopoulos, Phys. Rev. E 66 (2002) 055601(R).
[17] S.F. Mingaleev, A.E. Miroshnichenko, Y.S. Kivshar, Opt. Express 15 (2007) 12380.
[18] A.R. Cowan, J.F. Young, Phys. Rev. E 68 (2003) 046606.
[19] A.E. Miroshnichenko, S. Flach, Y.S. Kivshar, Rev. Mod. Phys. 82 (2010) 2257.
[20] Q.M. Ngo, K.Q. Le, V.H. Pham, L.D. Vu, J. Opt. Soc. Am. B 31 (2014) 1054.
[21] K. Nozaki, A. Shinya, S. Matsuo, T. Sato, E. Kuramochi, M. Notomi, Opt. Express 21 (2013) 11877.
[22] L.Y. Mario, S. Darmawan, M.K. Chin, Opt. Express 14 (2006) 12770.
[23] M. Heuck, P.T. Kristensen, Y. Elesin, J. Mørk, Opt. Lett. 38 (2013) 2466.
[24] G. D'Aguanno, D. de Ceglia, N. Mattiucci, M.J. Bloemer, Opt. Lett. 36 (2011) 1984.
[25] Y. Shuai, D. Zhao, Z. Tian, J.-H. Seo, D.V. Plant, Z. Ma, S. Fan, W. Zhou, Opt. Express 21 (2013) 24582.
[26] Y. Shuai, D. Zhao, A.S. Chadha, J.-H. Seo, H. Yang, S. Fan, Z. Ma, W. Zhou, Appl. Phys. Lett. 103 (2013) 241106.
[27] W. Suh, O. Solgaard, S. Fan, J. Appl. Phys. 98 (2005) 033102.
[28] Y.-G. Roh, T. Tanabe, A. Shinya, H. Taniyama, E. Kuramochi, S. Matsuo, T. Sato, M. Notomi, Phys. Rev. B 81 (2010) 121101(R).
[29] A. Taflove, Computational Electrodynamics, Artech House, Boston, 1995.
[30] A. Farjadpour, D. Roundy, A. Rodriguez, M. Ibanescu, P. Bermel, J. D. Joannopoulos, S.G. Johnson, G. Burr, Opt. Lett. 31 (2006) 2972.
[31] J.M. Laniel, N. Ho, R. Vallee, J. Opt. Soc. Am. B 22 (2005) 437.
[32] F. Verger, V. Nazabal, F. Colas, P. Němec, C. Cardinaud, E. Baudet, R. Chahal, E. Rinnert, K. Boukerma, I. Peron, S. Deputier, M. Guilloux-Viry, J.P. Guin, H. Lhermite, A. Moreac, C. Compère, B. Bureau, Opt. Mater. Express 3 (2013) 2112.
[33] R. Magnusson, M. Shokooh-Saremi, Opt. Express 15 (2007) 10903.
[34] Y. Kanamori, T. Kitani, K. Hane, Appl. Phys. Lett. 90 (2007) 031911.

Please cite this article as: Q.M. Ngo, et al., Optics Communications (2014), http://dx.doi.org/10.1016/j.optcom.2014.11.017